Robust Torque Control for Steer-by-Wire Vehicles

N. Bajcinca
Institute of Robotics and Mechatronics
German Aerospace Center, DLR
naim.bajcinca@dlr.de

M. Hauschild
Institute of Robotics and Mechatronics
German Aerospace Center, DLR
markus.hauschild@dlr.de

R. Cortesão
Institute for Systems and Robotics
University of Coimbra
cortesao@isr.uc.pt

Abstract

A force-feedback actuation loop for a steer-by-wire vehicle is developed. It is shown that the performance of this loop can be essentially improved by the introduction of a torque sensor. Partial model based control algorithms based on disturbance observer (DOB) and active observers (AOB) are applied to enhance the robustness vs. non-modelled dynamics and uncertain driver impedance. An additional PD control is added in the feed-forward loop to improve the driver feeling.

1 Introduction

Vehicle steering technology is evolving by substituting the mechanical and hydraulic subsystems with electrical equivalents to boost performance and enhance safety. *Steer-by-wire* is probably the most challenging steering technology, whereby a highly complex mechatronical system consisting of computing units, sensors and actuators replaces the mechanical interface (steering column) between the driver and vehicle. A steer-by-wire system is basically a *master-slave* system: the driver corresponds to the *operator*, the vehicle to the *environment*, the force-feedback actuator to the *master* and the front-wheel actuator to the *slave*. From the control point of view, a steer-by-wire system includes two force/position actuation inner-loops, which are coupled by a suitable outer-loop controller for the provision of a desired steering dynamics. This paper is concentrated on the force-feedback actuation loop.

The essential components of the force-feedback actuator used to apply the vehicle reaction torque on the driver are a servo-motor, a Harmonic-Drive gear and the torque sensor. At the present, automotive industry is rather reluctant in using Harmonic-Drive technology due to the cost matters and its torque ripples (see later).

There are virtually no literature results on torque control for steer-by-wire vehicles. Obviously, most approaches are based on open-loop model-based torque control algorithms, that is (due to cost matter) no torque sensors have been included in feedback actuation. However, the performance of such control strategies is limited since the torque applied to the driver is not sensed, thus lacking the compensation of friction, unmodelled dynamics and disturbances. This paper follows the closed-loop strategy by introducing a torque sensor at the steering wheel. The authors believe that a closed-loop approach of the torque inner-loop response improves essentially the driver feeling, it provides additional robustness to the overall steer-by-wire response and finally disburdens the outer-loop controller dynamics.

Due to considerable modelling errors and uncertainties, partial model-based control approach is applied, that is, instead of fitting the physical model into a mathematical one, the opposite is tempted, the physical model is forced to fit into a mathematical description, by introducing correction signals at the input. Therefore, the observer-based algorithms: Disturbance Observer (DOB), [8], [10] and Active Observer (AOB), [2] are used.

The paper is organized as follows. In Section 2 the force-feedback control in the context of the steer-by-wire system is discussed. In Section 3 the components of the the steer-by-wire test-bed are presented. Details about the hardware and modelling of the force-feedback actuator are discussed. Section 4 recalls the basic theory of the disturbance observer and Section 5 the basics of the active observer algorithm. Finally, Section 6 presents experimental results of the tests with DOB and AOB.

2 System modelling

Fig. 1 shows a simplified interaction scheme of the driver and a steer-by-wire vehicle via a force-feedback actuator. Notice that τ_d stands for the forces generated at the muscles of the driver, τ_r is the reaction torque which the driver should feel, δ_h is the steering angle and δ_s stands for the vehicle lateral position. The front-wheel actuation, vehicle dynamics reaction and the actuation coupling control is included within the *Steer-by-Wire Vehicle* block. The *Driver Impedance* block represents the passive biomechanical impedance of the driver arm[7]. It has been shown that the complex neuro-muscular phenomena may be roughly modelled by a stiffness and damping, which however are highly uncertain; e.g. in [6] it was shown that the human arm stiffness may vary between 2 Nm/rad and 600 Nm/rad.

The discussion of this paper focuses on the block *Force Feedback Actuation*. Its task is to apply the torque τ_r computed by the outer-loop steer-by-wire controller on the

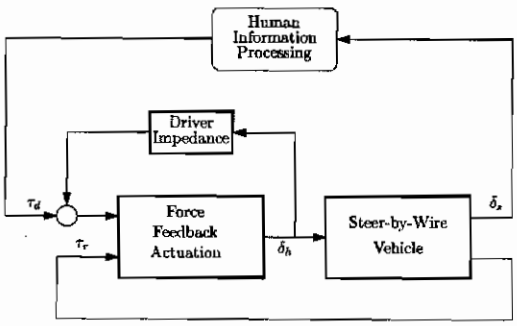

Figure 1: *Force-feedback in a steer-by-wire vehicle.*

driver. Basically, in a steer-by-wire system (and in general in force-feedback control) two approaches are possible. In the so-called *open-loop* force control, the torques applied on the driver are not sensed, i.e. a feed-forward control scheme is used. Its disadvantage is that in reality torque differs from the computed one, owing to several factors such as system noise, friction and inertia in the interface mechanism. To compensate for the above effects and improve control accuracy and performance, the interface needs to incorporate a torque sensor. This is usually called *closed-loop* force control in force-feedback literature [1]. In this paper the latter approach is applied.

The essential torque components measured by the sensor are included in the following equation,

$$\tau = P_l \tau_m - Z_{HD}\delta_h - (\tau_d + Z_{SW}\delta_h + Z_d\delta_h + \tau_{HD}), \quad (1)$$

whereby,

τ :	Measured torque,
P_l:	Linear torque transfer function,
τ_m:	Motor torque,
Z_{HD}:	Mechanical impedance of the force-feedback actuator,
Z_{SW}:	Scaled steering wheel impedance (inertia),
Z_d:	Driver impedance,
τ_{HD}:	Harmonic-drive periodic torque ripples.

The definition of P_l follows from (1). It represents the transfer function from the motor torque τ_m to the measured torque, while the steering wheel is kept fixed, $\delta_h = 0$. The Harmonic-Drive torque τ_{HD} exhibits nonlinear dependency on steering angle, its rate and motor torque, see Section 3, Fig. 5.

Model-based control approaches require good models for all these components, which is rather a difficult task. In addition, the driver impedance is Z_d is highly uncertain, since the driver may hold the steering wheel tight (high Z_d) or let it free ($Z_d = 0$). To overcome these problems, in this paper a partial model-based control approach will be used, that is, the components which are hard to model or are uncertain are considered simply as disturbances. Thus, the open-loop is described by the simple equation,

$$\tau = P_l \tau_m + \textit{disturbances}. \quad (2)$$

Notice that this is a simplified model of the torque balance, since it is implicitly assumed that the torque ripple τ_{HD} is additive, i.e. its dependency on τ_m is disregarded.

3 The Steer-by-Wire Setup

This section provides a description of steer-by-wire force-feedback actuator. In the sequel, the hardware components of the actuator are presented. This is followed by a discussion on its dynamics.

3.1 Harmonic Drive Gear

The main component in the the force-feedback actuator, Fig. 2, is Harmonic Drive's FHA Series Hollow-Shaft Aetuator. It consists of a sine-commutated AC servo motor with the built in incremental encoder and a Harmonic Drive gear reduction. In Fig. 3 the main components of the Harmonic Drive gear are shown. The teeth on the nonrigid Flexspline and the rigid Circular Spline arc in continuous engagement. Since the Flexspline has two teeth fewer than the Circular Spline, one revolution of the input causes relative motion between the Flexspline and the Circular Spline equal to two teeth. With the Circular Spline rotationally fixed, the Flexspline rotates in the opposite direction to the input at a reduction ratio equal to one-half the number of teeth on the Flexspline. This relative motion may be seen by examining the motion of a single Flexspline tooth over one-half an input revolution. The tooth is fully engaged when the major axis of the Wave Generator input is at 0°. When the Wave Generator's major axis rotates to 90°, the tooth is fully disengaged. Full reengagement occurs in the adjacent Circular spline tooth space when the major axis rotates 180° back to 0°, thereby producing the two tooth advancement per input revolution.

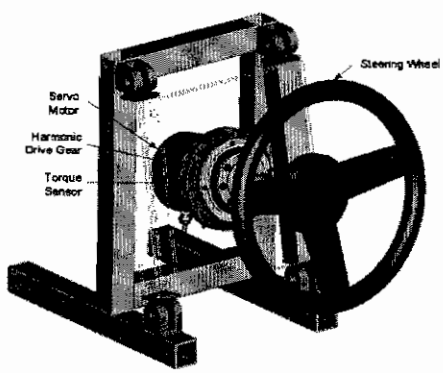

Figure 2: *Force-feedback actuator*

The steering wheel is mounted directly on the gear output shaft. Due to the high single stage gear reduction ratio of $N = 50$, a compact unit could be designed, that provides an output torque of up to approximately 50 Nm. Further advantages of the solution are that there is virtually no backlash and that Harmonic Drive gears are reversible and can be back-driven in an emergency.

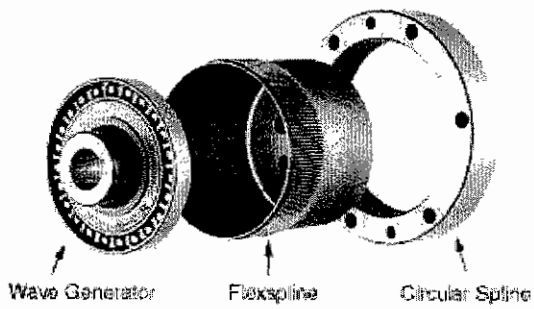

Figure 3: Harmonic Drive gear components

Various effeets such as friction, the torque ripple, typical for Harmonic Drive gears, and the motor's moment of inertia need to be compensated to provide a smooth steering feeling, comparable to the feeling of a mechanical steering mechanism of today's vehicles. Experiences from the light-weight robotics, whereby at each joint a torque sensor mounted on a Harmonie Drive gear has been used for feedback compensation, [9], encourage utilization of the same actuation technology for force-feedback on a steer-by-wire system. The inclusion of a torque sensor directly between the gear output and steering wheel therefore is suitable (see later) for closed loop compensation.

3.2 Torque Sensor

The funetion of the torque sensor is based on strain gauges. This operating principle implies that an additional elasticity is introduced into the mechanical system which accounts for approximately one third of the entire gear elastieity. The use of two independent measurement bridges provides redundancy and also allows the compensation of temperature ehanges and other disturbances.

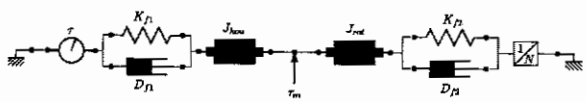

Figure 4: FHA model

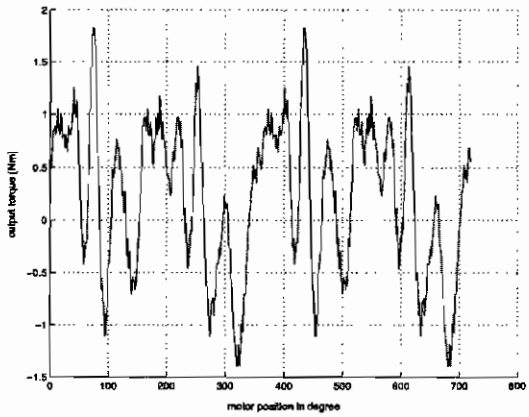

Figure 5: Torque ripple of the Harmonic Drive gear

3.3 Actuator Modeling

In [5] a model of the FHA actuator with the torque sensor is developed. In order to record step responses, the gear output is locked up mechanically when commanding motor current steps. It turns out that the measured gear output torque is surprisingly nonminimum-phase. A closer look at the setup explains this effect: in order to allow multiturn operation of the unit, without having the wiring problem of a rotating torque sensor, the torque is measured at the nonrotating gear housing. This torque does not only include the gear output torque, but also the motor torque. During the initial phase of a step response, the torque sensor registers the motor torque only, which builds up immediately. The gear output torque only gradually increases due to gear elastieities. Since the Harmonic Drive gear reverses the direction of rotation, the sensor registers a torque in the opposite direction and finally the gear output torque dominates the overall step response.

Fig. 4 depicts a simplified schematic model of the FHA actuator, allowing the verification of this behavior. It includes the moments of inertia of rotor and housing and the elasticities of torque sensor and Harmonic Drive gear, modelled as spring-damper systems. Thereby, it can be shown that the non-minimum phase zero in the model is caused by the elasticity of the strain gauges. Thus the nonminimal phase effeet is principally conditioned. However, this zero is not critieal, because of the high sensor stiffness.

N:	Gear reduetion ratio
D_{f1}:	Damping constant, sensor elasticity
K_{f1}:	Stiffness constant, sensor elasticity
D_{f2}:	Damping constant, gear elasticity
K_{f2}:	Stiffness constant, gear elasticity
J_{hou}:	Moment of inertia, motor housing
J_{rot}:	Moment of inertia, rotor.

Measurements with the joint in motion revealed further

unmodeled characteristics. Fig. 5 displays the torque ripple, which, as one of the most serious disturbances in the steering wheel setup, needs to be reduced through compensation. The gear's torque error is periodic in nature and its fundamental component corresponds to twice the frequency of the motor shaft speed. [4] analyzes the Harmonic Drive gear torque ripple and discusses the connection to the gear's mechanical operating principle.

4 DOB based control

The disturbance-observer control method uses the inverse model approach for the design of a two degree of freedom control architeeture [8], [10], by providing both, feedforward and feedback control. Its scheme is shown in Fig. 6. It can be shown that sensitivity $S(j\omega)$ and comple-

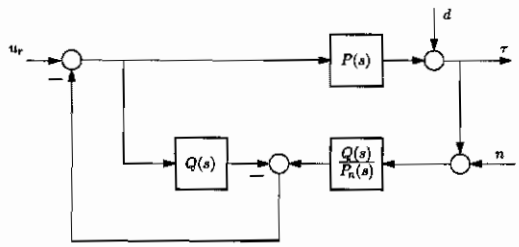

Figure 6: Disturbance observer scheme for force control.

mentary sensitivity $T(j\omega)$ functions of this structure are as follows,

$$S := \frac{\tau}{d} = \frac{1}{1+L} = \frac{P_n(1-Q)}{P_n + (P-P_n)Q} \tag{3}$$

$$T := -\frac{\tau}{n} = \frac{L}{1+L} = \frac{QP}{P_n + (P-P_n)Q}, \tag{4}$$

whereby the open-loop transfer function, L, is easily shown to be,

$$L = \frac{PQ}{P_n(1-Q)}. \tag{5}$$

Notice that the DOB structure introduces two functions, $P_n(s)$, which is called *nominal* (or *target*) plant and a filter $Q(s)$. The basic idea of the DOB approach is to force the behavior of the overall system in the operating frequency range be as that of the nominal plant P_n. Indeed, the transfer function from u_r to τ in the DOB scheme is,

$$\frac{\tau}{u_r} = \frac{PP_n}{P_n + (P-P_n)Q}, \tag{6}$$

which for the frequencies where $|Q(j\omega)| \approx 1$, tends to P_n. On the other side, notice that because of $S(j\omega) \to 0$, the system response on disturbances d is minimized at these frequencies, while the response is highly sensitive on measurement noise n, $T(j\omega) \to 1$. Fortunately in most applications the disturbance d is low frequent, while measurement noises are high-frequent. Therefore, for a given application the design task of the filter Q is to shape it in sueh a way that $|Q(j\omega)| \approx 1$ in the frequency range of interest (usually low frequencies), and to let it tend to zero $|Q(j\omega)| \to 0$ for higher frequencies for noise attenuation.

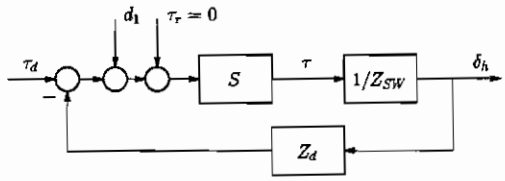

Figure 7: For the provision of a better feeling, T is supplied additional damping.

The essential task of a force-feedback algorithm is to provide the driver a good feeling. In Fig. 7 the mapping from the force generated in the muscles of the driver τ_d to the steering angle δ_h is schematically shown. Thereby, S stands for the sensitivity function (5) and d_1 includes motor inertia, harmonic drive inertia and its ripples, (1). In order to improve the driver feeling, the sensitivity function ST will be provided with additional damping. Thus, the scheme in Fig. 6 is augmented with an additional PD controller term as shown in Fig. 8, $C(s) = P + Ds$.

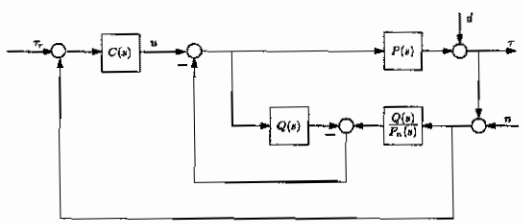

Figure 8: Disturbance observer scheme for force control.

5 AOB based control

A linear system represented in state space by

$$\begin{cases} x_{r,k} = \Phi_r x_{r,k-1} + \Gamma_r u_{k-1} \\ y_k = C_r x_{r,k}, \end{cases} \tag{7}$$

can be controlled through state feedback (e.g. optimal control, adaptive control, deadbeat control and "pure" pole placement control). In praetice, the main problem of this approach is that (7) does not represent exactly the real system. In fact, unmodeled terms including noise, higher order dynamics, parameter mismatches, couplings and un-

known disturbances are not addressed in the control design. Therefore, it is necessary to develop a control structure that can deal with them, so that the overall system may have the desired behavior. The AOB state space control design satisfies these requirements.

The main goal of the AOB is to fit a physical system (i.e. its input/output behavior) into a linear mathematical model, rather than to fit a mathematical model into a physical system. To accomplish this goal, a description of the system (closed loop and open loop) is necessary. A special Kalman Filter (KF) has to be designed. The motivation for this special KF is based on:

1. A desired closed loop system for the state estimation.
2. An extra equation to estimate an equivalent disturbance referred to the system input. An active state p_k (extra-state) is introduced to compensate unmodeled terms, providing a feedforward compensation action.
3. The stochastic design of the Kalman matrices Q and R for the AOB context. Model reference adaptive control appears if $Q_{x_{r,k}}$ is much smaller than Q_{p_k}. In this case, the estimation for the system state follows the reference model. Everything that does not fit in the $x_{r,k}$ model goes to p_k.

Section 5.1 describes the first-order AOB algorithm[1].

5.1 AOB-1 Algorithm

Controlling the system of (7) through state feedback from an observer and inserting p_k in the loop, the overall system can be described by

$$\begin{bmatrix} x_{r,k} \\ p_k \end{bmatrix} = \begin{bmatrix} \Phi_r & \Gamma_r \\ 0 & 1 \end{bmatrix} \begin{bmatrix} x_{r,k-1} \\ p_{k-1} \end{bmatrix} + \begin{bmatrix} \Gamma_r \\ 0 \end{bmatrix} u_{k-1} + d_k \tag{8}$$

and

$$y_k = C_a \begin{bmatrix} x_{r,k-1} & p_{k-1} \end{bmatrix}^T + n_k, \tag{9}$$

where

$$u_{k-1} = r_{k-1} - \begin{bmatrix} L_r & 1 \end{bmatrix} \begin{bmatrix} \hat{x}_{r,k-1} \\ \hat{p}_{k-1} \end{bmatrix}. \tag{10}$$

The stochastic inputs d_k and n_k represent respectively model and measure uncertainties. The state estimate of (8) is based on the desired closed loop (i.e. $\hat{p}_k = p_k$ and $\hat{x}_{r,k} = x_{r,k}$). It is

$$\begin{bmatrix} \hat{x}_{r,k} \\ \hat{p}_k \end{bmatrix} = \begin{bmatrix} \Phi_r - \Gamma_r L_r & 0 \\ 0 & 1 \end{bmatrix} \begin{bmatrix} \hat{x}_{r,k-1} \\ \hat{p}_{k-1} \end{bmatrix} + \begin{bmatrix} \Gamma_r \\ 0 \end{bmatrix} r_{k-1} + K_k(y_k - \hat{y}_k), \tag{11}$$

[1]The general AOB algorithm uses N extra states to describe p_k [3], [2].

with

$$\hat{y}_k = C_a \left(\begin{bmatrix} \Phi_r - \Gamma_r L_r & 0 \\ 0 & 1 \end{bmatrix} \begin{bmatrix} \hat{x}_{r,k-1} \\ \hat{p}_{k-1} \end{bmatrix} + \begin{bmatrix} \Gamma_r \\ 0 \end{bmatrix} r_{k-1} \right) \tag{12}$$

and

$$C_a = \begin{bmatrix} C_r & 0 \end{bmatrix}. \tag{13}$$

The Kalman gain K_k reflects the uncertainty associated to each state based on model and measure uncertainties. It is computed from

$$K_k = P_{1k} C_a^T \left[C_a P_{1k} C_a^T + R_k \right]^{-1}, \tag{14}$$

with

$$P_{1k} = \Phi_n P_{k-1} \Phi_n^T + Q_k \tag{15}$$

and

$$P_k = P_{1k} - K_k C_a P_{1k}. \tag{16}$$

Φ_n is the augmented open loop matrix,

$$\Phi_n = \begin{bmatrix} \Phi_r & \Gamma_r \\ 0 & 1 \end{bmatrix}. \tag{17}$$

Q_k is the system noise matrix and represents model uncertainty. It is given by

$$Q_k = \begin{bmatrix} Q_{x_{r,k}} & 0 \\ 0 & Q_{p_k} \end{bmatrix}. \tag{18}$$

The measurement noise matrix R_k represents measure uncertainty. P_k is the mean square error matrix. Its initial value should reflect at least the uncertainty in the state estimation. It should not be lower than the initial matrix Q_k.

6 Experimental results

DOB algorithm. This section brings the experimental results with the DOB algorithm. A fourth order target plant P_n with four poles near to the identified system is used to compensate the linear dynamics P_l, (1), of the force-feedback actuator, (6),

$$P_n = \frac{1.132e011}{s^4 + 365.3s^3 + 155110s^2 + 2.399e007s + 3.773e009}. \tag{19}$$

Notice that the non-minimum phase zero of the plant is excluded from the target plant. As a $Q-$filter a fourth-order Butterworth filter is used,

$$Q = \frac{w_q^4}{s^4 + 2.6132w_q s^3 + 3.414w^2 s^2 + 2.6132w_q^3 s + w_q^4}, \tag{20}$$

with $w_q = 190$.

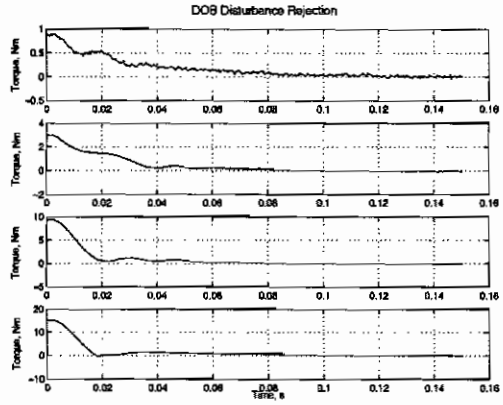

Figure 9: *Disturbance rejection of the DOB control with* $Z_d \rightarrow \infty$.

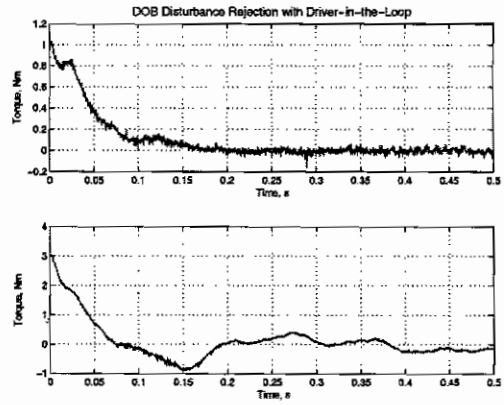

Figure 10: *Disturbance rejection of the DOB control with the driver-in-the-loop.*

Fig. 9 shows the rejection of step disturbances of different levels applied at the output. Thereby the steering wheel is kept fixed, $\delta_h = 0$, that is, an infinite driver impedance is emulated. In Fig. 10 these experiments are repeated with the human-in-the-loop, that is, the responses of the system on step disturbances during the normal driving operation are shown. These experiments prove the robustness of the algorithm w.r.t the impedance of the driver.

Fig. 11 and Fig. 12 show torque tracking responses of sinusoidal torque inputs of different frequencies, respeetively with an infinite driver impedance (steering-wheel kept fixed) and with driver-in-the-loop.

Experimental tests verify that the performanee of the force-feedbaek actuation improves the driving feeling for different maneuvers such as abrupt steering. This is due to the high-bandwidth of the torque control. In addition, the torque ripples of Harmonic Drive gear are compensated.

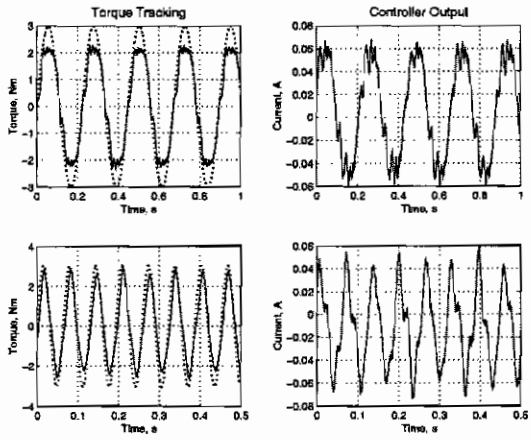

Figure 11: *Torque tracking responses for* $Z_d \rightarrow \infty$.

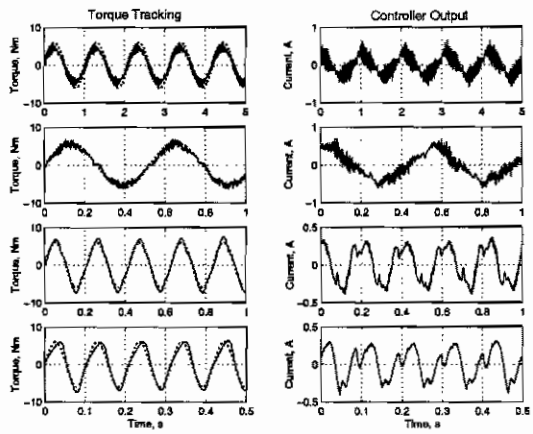

Figure 12: *Torque tracking responses with driver-in-the-loop.*

AOB algorithm. Fig. 13 and Fig. 14 exhibit the disturbance rejection and the tracking performance of the AOB algorithm. Note the compensating response of the active state.

7 Conclusions

A high bandwidth force actuation system for steer-by-wire vehieles is presented in this paper. Rather than open-loop force control, the elosed-loop force control strategy is followed by installing a torque sensor in the force-feedback actuator. The partial model based control approach is used, that is, instead of putting effort in modelling the processes, which are difficult to model (e.g. torque ripples in the harmonie drive gear) or are highly uneertain (driver impedance), observer-based algorithms are used to caneel the non-modelled physical dynam-

ics. Thereby, the disturbance-observer (DOB) and active-observer (AOB) control has been applied. While a certain reluetance in applying the harmonic-drive gearing technology because of the torque ripples is at the present noticeable, this paper shows tbat at the expense of an additional torque sensor, high-bandwidth robust and smooth torque control is feasible. Zero-torque regulation problem is proposed to judge about the steering feeling. It is shown that a PD controller in the feed-forward loop provides improvement (damping) of the steering feeling.

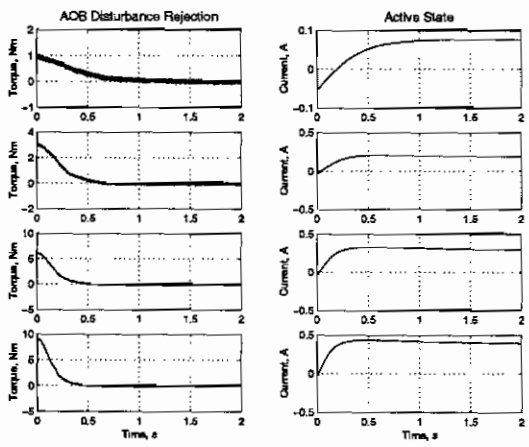

Figure 13: *Disturbance rejection of AOB for* $Z_d \rightarrow \infty$.

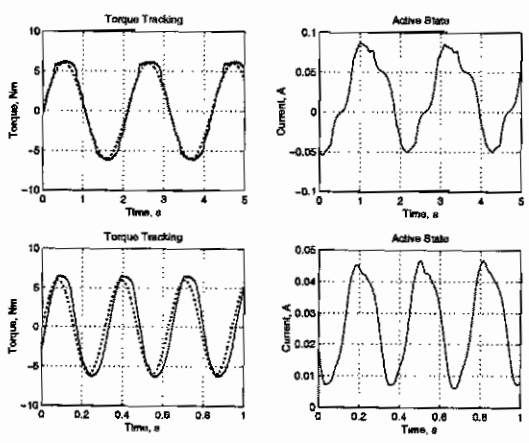

Figure 14: *Torque tracking of AOB for* $Z_d \rightarrow \infty$.

References

[1] Grigore C. Burdea. *Force and Touch Feedback for Virtual Reality*. John Wiley, 1996.

[2] R. Cortesão. *Kalman Techniques for Intelligent Control Systems: Theory and Robotic Experiments*. PhD thesis, University of Coimbra, 2003.

[3] R. Cortesão, R. Koeppe, U. Nunes, and G. Hirzinger. Compliant motion control with stochastic active observers. In *Proc. of the Int. Conf. on Intelligent Robots and Systems (IROS)*, pages 1876–1881, USA, 2001.

[4] F. Ghorbel. On the kinematic error in harmonic drive gears. *Transactions of the ASME, Journal of Mechanical Design*, (123):90–97, 2001.

[5] M. Hauschild. *Torque Control of the Harmonic Drive Gear using the DLR Torque Sensor*. Diploma Thesis, Institute of Robotics and Mechatronics, DLR, 2002.

[6] N. Hogan. Controlling impedance at the man/machine interface. *Proc. of the IEEE Int. Conference on Robotics and Automation*, 1989.

[7] R. Koeppe. *Robot Compliant Motion based on Human Skill*. PhD thesis, Swiss Federal Institute of Technology, 2001.

[8] K.Ohnishi. A new servo method in mechatronics. *Trans. Japonese Society of Electrical Engineering*, 107-D:83–86, 1987.

[9] A. Albu Schäffer. *Regelung von Robotern mit elastischen Gelenken am Beispiel der DLR-Leichtbauarme*. PhD thesis, Institute of Robotics and Mechatronics, DLR, 2001.

[10] K. Umeno and Y. Hori. Robust speed control of DC servomotors using modern two degrees-of-freedom controller design. *IEEE Trans. Industrial Electronics*, pages 363–368, 1991.